The effects of aggregated land cover data on estimating NPP in northern Wisconsin

Douglas E. Ahl[a],*, Stith T. Gower[a], D. Scott Mackay[b], Sean N. Burrows[a],
John M. Norman[c], George R. Diak[d]

[a]Department of Forest Ecology and Management, 120 Russell Laboratories, 1630 Linden Drive,
University of Wisconsin-Madison, Madison, WI, 53706, United States
[b]Department of Geography, 105 Wilkeson Quad, University at Buffalo, Buffalo, NY, 14261, United States
[c]Department of Soil Science, 1525 Observatory Drive, University of Wisconsin-Madison, Madison, WI, 53706, United States
[d]Space Science and Engineering Center, W. Dayton Street, University of Wisconsin-Madison, Madison, WI, 53706, United States

Abstract

Ecosystem models are routinely used to estimate net primary production (NPP) from the stand to global scales. Complex ecosystem models, implemented at small scales (<10 km^2), are impractical at global scales and, therefore, require simplifying logic based on key ecological first principles and model drivers derived from remotely sensed data. There is a need for an improved understanding of the factors that influence the variability of NPP model estimates at different scales so we can improve the accuracy of NPP estimates at the global scale. The objective of this study was to examine the effects of using leaf area index (LAI) and three different aggregated land cover classification products–two factors derived from remotely sensed data and strongly affect NPP estimates–in a light use efficiency (LUE) model to estimate NPP in a heterogeneous temperate forest landscape in northern Wisconsin, USA. Three separate land cover classifications were derived from three different remote sensors with spatial resolutions of 15, 30, and 1000 m. Average modeled net primary production (NPP) ranged from 402 gC m^{-2} year^{-1} (15 m data) to 431 gC m^{-2} year^{-1} (1000 m data), for a maximum difference of 7%. Almost 50% of the difference was attributed each to LAI estimates and land cover classifications between the fine and coarse scale NPP estimate. Results from this study suggest that ecosystem models that use biome-level land cover classifications with associated LUE coefficients may be used to model NPP in heterogeneous land cover areas dominated by cover types with similar NPP. However, more research is needed to examine scaling errors in other heterogeneous areas and NPP errors associated with deriving LAI estimates.
© 2005 Elsevier Inc. All rights reserved.

Keywords: Net primary production; Leaf area index; Light use efficiency; Absorbed radiation; Classification; Remote sensing

1. Introduction

Net primary production (NPP) is an important proxy for the metabolism of the biosphere, and therefore warrants accurate assessment. Model estimates of global NPP, the annual net uptake of carbon from the atmosphere, range from 40 to 80 PgC year^{-1}, indicating a large uncertainty (Cramer et al., 1999). Running et al. (1999) suggested the variation of three factors deserve further study in the context of using remote sensing to derive spatial estimates of NPP: 1) spatial resolution 2) land cover and 3) light use efficiency (LUE) estimates. An improved understanding is needed of how each of these factors and their interaction affect NPP estimates derived from ecosystem models.

In this paper we examine the influence of aggregated land cover information with estimates of leaf area index (LAI) to estimate NPP using a LUE model. For LUE models

(Monteith, 1972, 1977), NPP is a function of absorbed photosynthetically active radiation (APAR) and a LUE coefficient (ε) such that:

$$NPP = \varepsilon APAR \tag{1}$$

The LUE model is widely used to estimate NPP at large scales because it is conceptually simple and can be directly parameterized with remote sensing data (Bartelink et al., 1997; Choudhury, 2001; Coops et al., 1998; Franklin et al., 1997; Goetz & Prince, 1998; Gower et al., 1999; Landsberg & Gower, 1997; Medlyn, 1998; Running et al., 1994).

LAI, leaf area per unit ground area, is an important input to many simulation models that estimate the exchange of mass and energy between the terrestrial ecosystem and the atmosphere (Gower et al., 1999). LAI is correlated ($r^2 = 0.55 - 0.97$) to vegetation indices (VI) derived from remotely sensed data (Fassnacht et al., 1997; Running et al., 1986; Spanner et al., 1994). However, there is considerable variation in estimating LAI from a VI due to several biophysical factors, including species differences and sensor characteristics (Turner et al., 1999).

A method for calculating APAR from LAI involves determining the fraction of absorbed light (f_{APAR}) from the following:

$$f_{APAR} = 1 - e^{(-k\ LAI)} \tag{2}$$

where k is the light extinction coefficient describing the fraction of light intercepted by a leaf or canopy given the leaf distribution and sun angle (Campbell & Norman, 1998). Alternatively, APAR can be estimated empirically from a VI. Myneni and Williams (1994) concluded that f_{APAR} was approximately equal to the normalized difference vegetation index (NDVI). Reliable estimates of LAI and f_{APAR} are essential to model biogeochemical cycles and the effects of vegetation characteristics need to be quantified in scaling and validation efforts (Milne & Cohen, 1999).

Detailed models of ecosystem processes are often implemented over large areas in which direct measurements of many vegetation parameters are not feasible. Examples of models of this type are SiB2 (Sellers et al., 1996), IBIS (Foley et al., 1996), and BIOME-BGC (Running & Hunt, 1993). A key requirement for these models is vegetation type or land cover, which can be derived from the remotely sensed data (Thomlinson et al., 1999). The International Geosphere-Biosphere Program (IGBP) land cover scheme is a coarse scale classification that uses biome descriptions (e.g., deciduous broadleaf forest) such that each tree species can be composited into a biome-level IGBP class. Thomlinson et al. (1999) noted that ambiguities of translating between schemes arise because of the natural variability on the ground, which cannot be categorized into one generalized class type.

Many studies have examined the effects of aggregating spatial resolution from small grain size (high resolution) to large grain size (low resolution), and how it may affect various ecosystem processes (Benson & MacKenzie, 1995; He et al., 2002; Turner et al., 2000). Turner et al. (1996) showed that the accuracy of estimating NPP from remotely sensed data was inversely correlated to sensor resolution. They showed a 10% increase in simulated NPP values as sensor resolution aggregated from 1 to 50 km in Oregon. Discrepancy may be reduced by taking into account the vegetation present within coarse pixels. Turner et al. (1996) suggested that issues related to mixed pixels at the MODIS (250–500 m) scale need to be addressed. Reich et al. (1999) examined the effects of reduced pixel resolution on estimates of NPP by applying a modal filter to a fine scale (25 m grid) classification similar to the site-specific scheme described above. The NPP estimate was only 5% greater for a 1000 m resolution grid than a 25 m grid. Reich et al. (1999) suggested that as scale increases, the patchy nature of a heterogeneous landscape disappears with a proportionate impact to NPP. The study demonstrated the need to understand how grain size affects NPP estimates. Our study used existing data (e.g., land cover classification) derived from multiple sensor types rather than a neighborhood function (i.e. majority filter) to simulate varying resolution.

The objectives of this study were to determine the aggregation effects of using different land cover classification and LAI data on estimating NPP. We hypothesized that estimates of NPP would differ significantly among different land cover and leaf area spatial scales. We used three different land cover products that encompass a range in scale of vegetation classification scheme derived from high and low resolution remote sensors. In addition, we used three different LAI maps derived from three different methods. Differences in estimates of average NPP using a LUE model are presented and discussed.

2. Methods

2.1. Study site

The study area is an Earth Observing System (EOS) Validation site (http://landval.gsfc.nasa.gov/) centered on a 447-m tall communications tower (WLEF tower; 45.9450°N, 90.2733°W) in northern Wisconsin, USA. The topography is slightly rolling with an elevation difference of 45 m between highest and lowest elevations. The climate is cool, temperate continental, with mean air temperatures ranging from −12 to 19 °C for January and July, respectively. Average precipitation is 811 mm/year for this region (Barish & Meloy, 2000).

Much of northern Wisconsin, including the study area, was logged in the late 1800s–early 1900s and a heterogeneous mixture of forest cover types has regrown, reflecting a combination of complex glacial history and forest management (Fassnacht & Gower, 1997). Outwash, pitted outwash, and moraines comprise almost 63% of the geomorphic landform for this study site. Red pine plantations (*Pinus*

Table 1
Summary of the primary data sets used in this study

Data	Year collected	Reference
Micrometeorological	2000	Davis et al., 2003
PAR		
Air temperature		
Soil moisture		
Leaf area index	2000	Burrows et al., 2002
Plot tree inventory	1998	Burrows et al., 2002
Light use efficiency	2000	Ahl et al., 2004
Land cover		
WISCLAND	1993, 1994	Lillesand et al., 1998
ATLAS	1998	This study
MODIS	2000	GES, 2005

resinosa Ait.) dominate well drained glacial outwash. Northern hardwood species occur on fine textured moraines and include sugar maple (*Acer saccharum* Marsh.) and basswood (*Tilia americana* L.) primarily. Trembling aspen (*Populus tremuloides* Michx.) and balsam fir (*Abies balsamea* (L.) Mill.) dominate intermediate sites in this area. Poorly drained lowland organic soils (peat) comprise approximately 30% of the area and are dominated by speckled alder (*Alnus rugosa* DuRoi), white cedar (*Thuja*

occidentalis L.), and tamarack (*Larix laricina* DuRoi), with some balsam fir and black spruce (*Picea mariana* Mill.) throughout. Wetland grass, shrub and open water communities comprise less than 10% of the area.

An extensive field survey grid of 312 plots was established to estimate the spatial variability of leaf area index (LAI), land cover, and NPP for an area covering approximately 3.2×4.2 km (Burrows et al., 2002, 2003). LAI from these plot data ranged from 1.0 to 8.0 $m^2 m^{-2}$, and averaged 3.6 (Burrows et al., 2002).

2.2. Research design

Several diverse datasets were used in this research (Table 1). LAI data were collected at 205 of the 312 plots (Fig. 1) in 2000 and used to derive LAI maps. Land cover data were collected at 277 plots in 1998 and used for assessing the accuracy of land cover classifications. The effects of aggregated land cover information and spatial LAI data on landscape NPP estimates were evaluated using a LUE model among nine NPP estimation scenarios (Fig. 2). The approach to estimate NPP was to partition the site by land cover class. Three land cover maps were developed
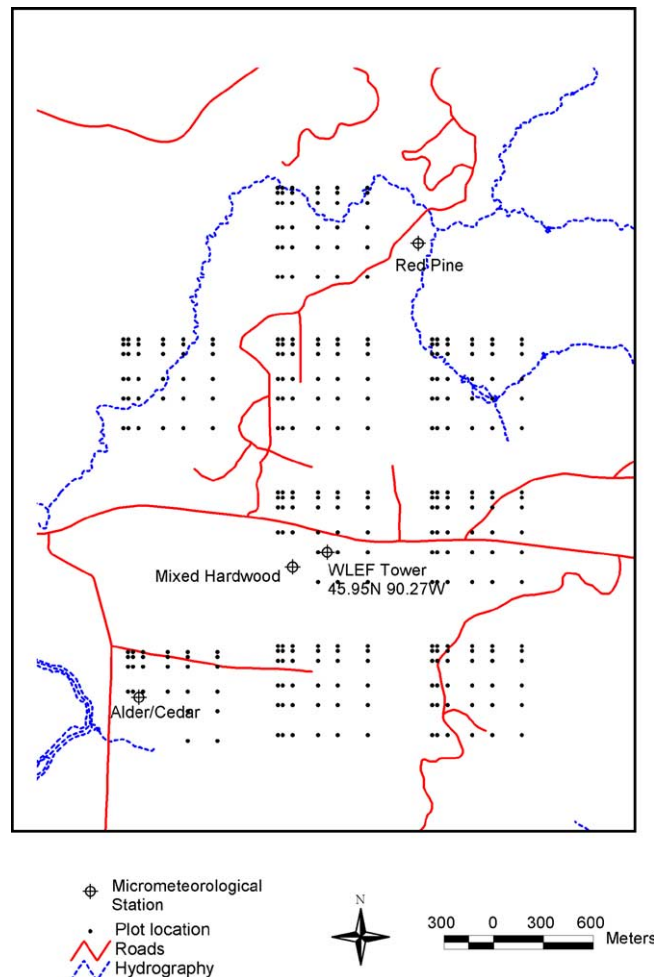

Fig. 1. Northern Wisconsin, USA, site location with 312 plot locations used as a source for LAI mapping and to assess land cover classification accuracy.

Land Cover From Remote Sensing, $\underline{X}$ **Field Based Leaf Area Index, $\underline{Z}$**

15m $\underline{A}$TLAS

30m $\underline{W}$ISCLAND

1km $\underline{M}$ODIS

$\underline{A}$veraged

30m $\underline{K}$riged

30m Co-Kriged $\underline{R}$emote Sensing

Single Pixel NPP Calculation

$$NPP_{XZ} = \varepsilon_x \, (1\text{-}e^{(-k\,LAI_z)}) \, PAR_{GS}$$

Separate Spatial NPP Estimates, XZ

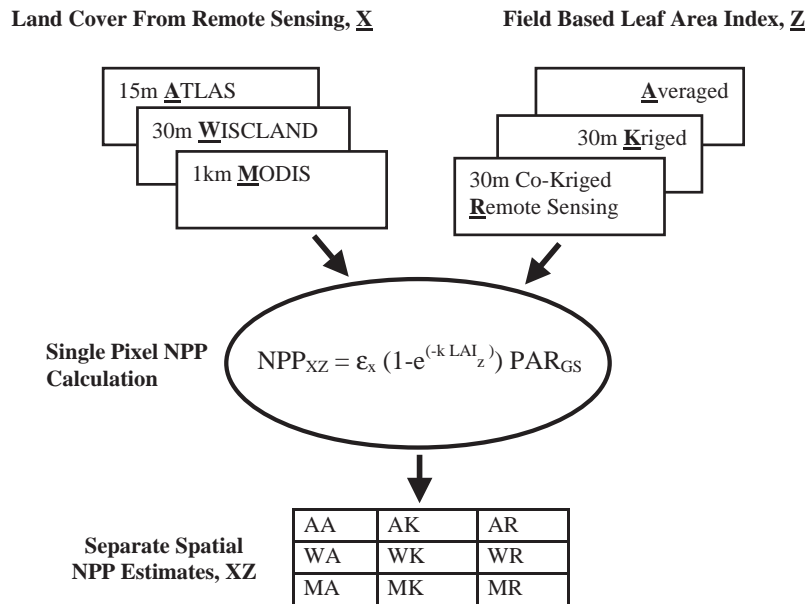| AA	AK	AR
WA	WK	WR
MA	MK	MR

Fig. 2. Conceptual diagram showing methodology for producing the nine different net primary production (NPP) maps in this study. Land cover is represented by three products: ATLAS, WISCLAND, MODIS. LAI is represented by three products: Average, Krige, Co-Krige with Remote Sensing. NPP is derived for each combination using a land cover specific light use efficiency (LUE) coefficient.

separately using the Airborne Terrestrial Land Applications Sensor (ATLAS), Landsat, and MODIS sensors (Table 1). The spatial resolution of ATLAS, Landsat, and MODIS in this study were 15 m, 30 m, and 1 km, respectively. The ATLAS and Landsat were classified using a site-specific classification scheme. The MODIS data were classified using the IGBP scheme (Table 2). Within each land cover class, LAI was estimated separately using 1) the mean LAI value for the class determined from the field data, 2) a kriged estimate of LAI, and 3) a co-kriged estimate of LAI. The two kriged LAI maps were created separately using field based LAI measurements. One LAI map was created using kriging constrained by the ATLAS land cover classification (Burrows et al., 2002). The second LAI map

was created using co-kriging with the ATLAS land cover classification and imagery from ATLAS and Landsat. The nine NPP maps were created from an LUE model by pairing each of three land cover maps with each of three methods for representing LAI. The LUE coefficient was also partitioned by land cover class for each scenario using mean coefficient values for each class taken from Ahl et al. (2004). The mean NPP for the nine scenarios were tested for significant differences against the highest resolution map NPP estimate.

2.3. Field data

A detailed description of the systematic plot design and inventory can be found in Burrows et al. (2002). All trees greater than 2.5 cm diameter at breast height (1.37 m) were identified using variable radius plots at each of the 277 plots. Each plot was assigned a site-specific class that could be collapsed into a IGBP land cover type (Table 2). Ahl et al. (2004) summarized the criteria used to assign plot data to a land cover class.

LAI was measured at each plot using a Li-Cor LAI-2000 Plant Canopy Analyzer (Li-Cor Inc., Lincoln, NE). Standard field measurement methods were used (Gower & Norman, 1991). Details of the measurements and methods used are described in Burrows et al. (2002). The average LAI was calculated for each land cover type and classification scheme (Table 2).

Prior to remote sensing image acquisition, eight 6×6 m ground targets were established in the WLEF study area for image georectification. Coordinates for the targets were determined using an Ashtech GG-24 Surveyor (Magellan Inc., Sunnyvale, CA) Global Positioning System (GPS).

Table 2
Adaptation of the site-specific and IGBP classification schemes (Thomlinson et al., 1999) used in this study with corresponding light use efficiency (LUE) and average leaf area index (LAI) values

Site-specific	LUE[a]	LAI[b]	IGBP	LUE	LAI
Aspen	0.51	4.0	Deciduous broadleaf	0.53	3.9
Forested wetland	0.41	4.1	Mixed	0.42	4.1
Northern hardwood	0.56	3.8	Deciduous broadleaf	0.53	3.9
Red pine	0.50	5.1	Evergreen needleleaf	0.41	4.5
Upland conifer	0.35	3.8	Evergreen needleleaf	0.41	4.5
Open wetland[c]	0.27	2.7	Wetland	0.27	2.7
Grass/shrub[c]	0.30	1.0	Grassland	0.3	1.0
Cropland[c]	3.0	3.5	Cropland	3.0	3.5

LUE (gC MJ^{-1}) and hemispherical LAI (m^2 leaf area m^{-2} ground area) values for the IGBP classes represent the mean of corresponding site-specific values.
 [a] LUE values of forest cover types taken from Ahl et al. (2004).
 [b] LAI values of cover types except cropland taken from Burrows et al. (2002).
 [c] LuE values taken from Gower et al. (1999).

Additional ground control points (GCPs) were collected with the GPS throughout the study area at features recognizable on the imagery. These features consisted primarily of road intersections. The relative accuracy of the GCPs, determined from a local survey benchmark, was ±50 cm.

2.4. Micrometeorological measurements

Micrometeorological data (photosynthetically active radiation (PAR), wind speed, temperature, precipitation, soil moisture, and relative humidity) were recorded every 15 min at the WLEF tower and hourly averaged data were stored (Table 1). Diurnal PAR were summed to derive a daily value. Gaps in the data were filled with PAR data collected at another site approximately 10 km away (Ewers et al., 2002). Temperature, soil moisture and understory PAR were available at three additional sites within 2.5 km of the WLEF tower located in stands dominated by mixed hardwoods, red pine, alder/cedar respectively (Fig. 1).

2.5. Imagery collection and preprocessing

Airborne multispectral data were collected using the ATLAS sensor (Brannon et al., 1994) on September 10, 1998 (Figs. 3 and 4a). ATLAS is a 14 channel sensor with 6 of the channels similar in spectral bandwidth to the Thematic Mapper (TM) and the Enhanced Thematic Mapper (ETM+) onboard the Landsat satellites. Data were collected at two different altitudes to produce nominal ground resolutions of 3 and 15 m respectively. All images were collected from 11:00 to 13:00 (CST) on a clear day. The images were georeferenced with ERDAS Imagine software (ERDAS Inc., 2000, Atlanta) using GCPs and a second order polynomial to relate the image coordinates to the GCP coordinates ±one pixel. The images were

resampled using a cubic convolution method. Other resampling methods (e.g., nearest neighbor) were examined but did not produce more accurate results.

2.6. Image classification procedure

The 15 m resolution ATLAS data were chosen for the classification because the entire study site was contained within one swath of the flight line, which eliminated the need to combine multiple flight lines and reduced the errors associated with aircraft distortion. A semi-automated classification using a subset of the red, near-infrared, and mid-infrared bands and NDVI was employed (Lillesand & Keifer, 2000). To reduce misclassification of forested wetlands, wetlands were separated in the imagery from uplands using the Wisconsin DNR wetland survey (Lillesand et al., 1998; Sader et al., 1995).

We used hybrid image classification techniques (Bauer et al., 1994; Lillesand & Keifer, 2000; Stuckens et al., 2000) to classify the ATLAS imagery using the site-specific classification scheme (Table 2). A post classification contextual procedure was applied to remove the "salt and pepper" effect and assign each pixel a majority land cover of the classes surrounding it (Stuckens et al., 2000). To assist in refining the wetland/upland delineation further, soils data (U.S. Forest Service, Dave Hoppe, unpublished data) were used to identify potential wetland areas not identified on existing wetland maps. Several field visits provided additional information on potential classification errors, which were corrected using on-screen digitizing.

2.7. WISCLAND data

We used the WISCLAND land cover product (Lillesand et al., 1998) to represent a land cover classification derived from the Landsat satellite (Figs. 4b and 5b). We chose this

a) ATLAS 15m 1998   b) Landsat5 TM 30m 1994   c) MODIS 500m 2001
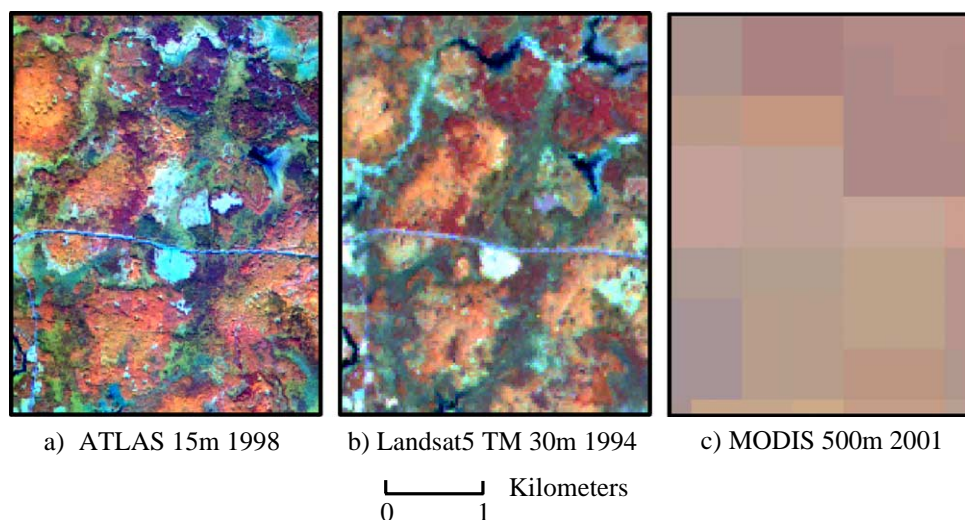
Kilometers

0   1

Fig. 3. Representative leaf-on imagery for the study site from a) ATLAS, b) Landsat TM, and c) MODIS with spatial resolution and year of imagery indicated. The circular clearing in the middle of the ATLAS and TM images is the location of the WLEF communications tower.
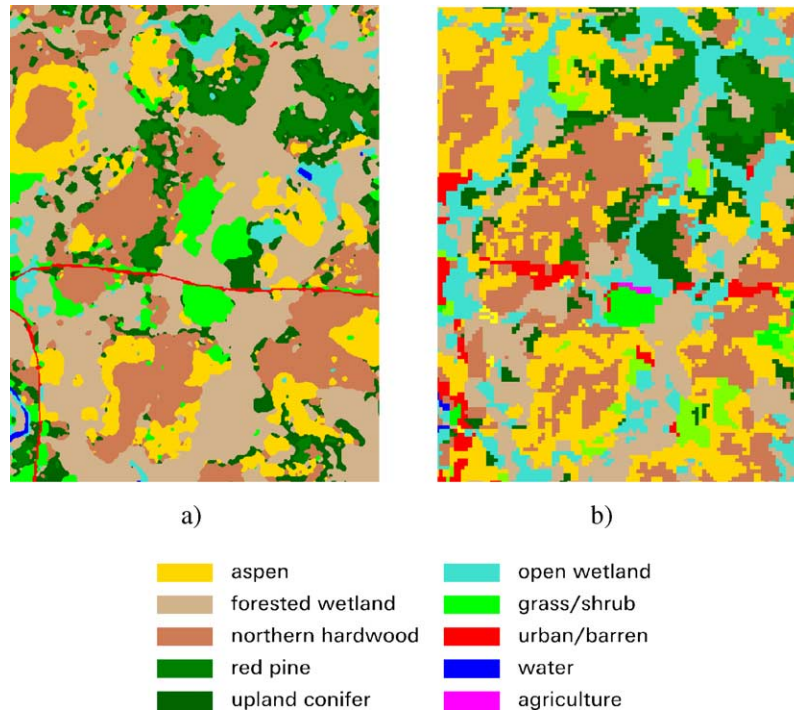
Fig. 4. Land cover classifications from a) ATLAS and b) WISCLAND land cover product (Lillesand et al., 1998).
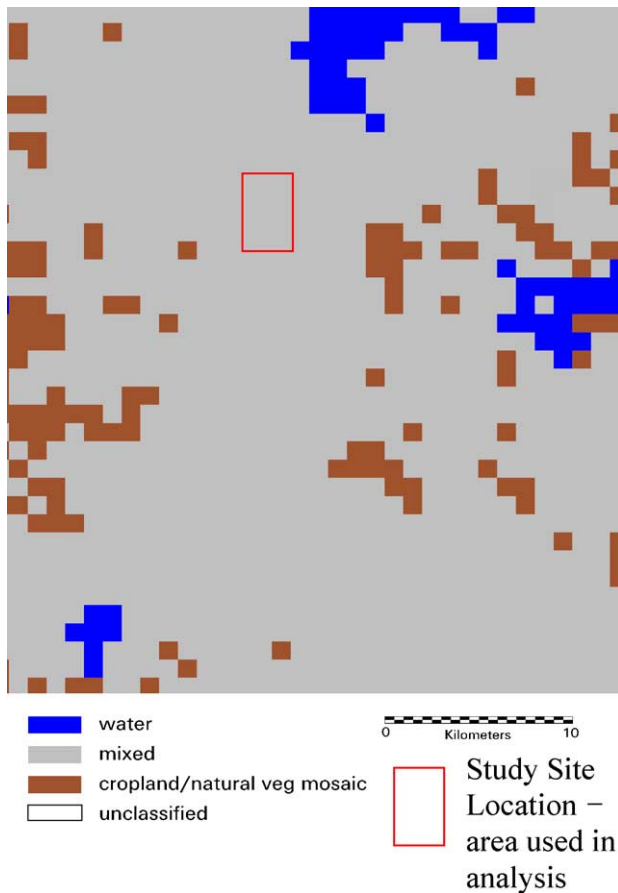

Fig. 5. MODIS land cover classification product obtained through GES Data and Information Services Center (2005).

product for three reasons: 1) it represents a publicly available product at a site-specific classification level, 2) other Landsat imagery at the time of analysis were unusable because of excessive clouds or haze, and 3) it was an independently derived land cover product. The WISC-LAND product was based on early 1990's imagery, but the WISCLAND classification was similar to the site-specific classification scheme.

2.8. MODIS imagery and data

MODIS imagery (MOD09) was obtained on July 13, 2001 encompassing study site (Fig. 4c). MODIS is a 36 channel sensor divided among three spatial resolutions: 250, 500, and 1000 m. The spectral bandwidth of the bands primarily used for land-based applications are only slightly different from that of Landsat ETM+. The 500 m resolution image was subset for the study area and classified using the IGBP scheme and the same classification techniques described for ATLAS data.

The MODIS 1 km land cover product (MOD12Q1) was the coarsest scale in this study (Fig. 6) and was obtained from the GES DISC (GES Data and Information Services Center, 2005). These MODIS data were classified using the IGBP classification scheme. The classification should be viewed as preliminary and is still under evaluation. At the time of this analysis, collection V004 was not available. However, subsequent analysis with V004 data show that our classification of the 500 m data and land cover product of MOD12 did not change.
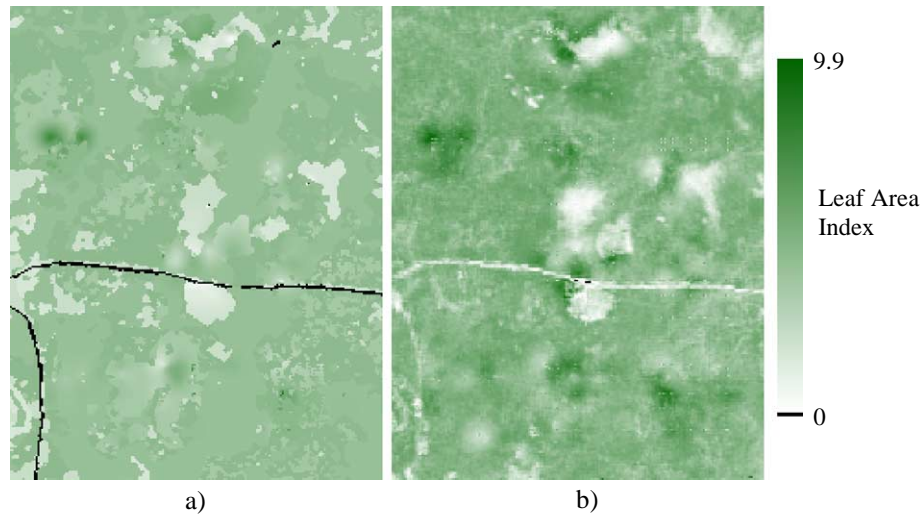
Fig. 6. One-sided leaf area index (LAI) maps derived using a) kriging with land cover information and b) co-kriging with land cover and remote sensing normalized difference vegetation index (NDVI) data. Mean, standard deviation, and range is 3.9, 0.9, and 0–8.8 for a) and 3.4, 0.9, and 0–9.6 for b).

2.9. Land cover classification accuracy assessment

The ATLAS and WISCLAND land cover classifications were compared to the inventory plots to perform the accuracy assessment using standard techniques (Congalton, 1991; Lillesand & Keifer, 2000). An error matrix was created from the plots and used to compute overall, user's and producer's accuracy measures (Lillesand & Keifer, 2000).

We did not assess the accuracy of the MODIS products because of the lack of variation within the site (i.e., the entire site is labeled a mixed forest category). A qualitative examination using the field inventory data revealed that the 500 m and 1 km MODIS land cover products represented the land cover of the site very well at that scale. Only one MODIS product (1 km) was used in subsequent analyses because the 500 m and 1 km classifications were identical.

2.10. Spatial LAI

The coordinates of the field plots were determined from a cyclic sampling design, which was implemented to characterize the vegetation cover and LAI of a 13 km^2 area centered on the WLEF Tower (Burrows et al., 2002) (Fig. 1). The purpose for implementing the cyclic design was to maximize the information available to subsequent analyses concerning vegetation characteristics in this heterogeneous landscape. The design optimized the location of the plots so plot information such as LAI could be used in geostatistical analyses such as spatial regression and kriging, which also allowed for the incorporation of covariates such as remotely sensed data and land cover (Burrows et al., 2002; Cressie, 1993; Pinheiro & Bates, 2000).

The SAS/MIXED® software (SAS Institute Inc., 2000) was used to construct a map of LAI from the LAI plot data and the ATLAS classification with a kriging function (Burrows et al., 2002). Kriging uses a weighted average function to predict values at new locations based on a semivariogram and LAI measured at other locations (Cressie, 1993). Each land cover type had a spherical spatial covariance structure based on the LAI measurements, which were specified for the kriging function in SAS/MIXED® (Burrows et al., 2002).

A second LAI map was created using the same information and procedure just described but also incorporated information from the ATLAS imagery and Landsat ETM+ imagery (Landsat imagery acquired October 6, 1999). This kriging procedure is refered to as co-kriging (Cressie, 1993) and takes advantage of the LAI and imagery observations at each plot. We first transformed the imagery using a canonical components transformation to (i) reduce the dimensionality of the data (i.e., the number of bands used in processing) and (ii) help maximize LAI separability among land cover classes (Jakubauskas, 1996; Lillesand & Keifer, 2000). We used the first canonical variate in the co-krige function. Jakubauskas (1996) showed that the first canonical variate calculated from all Landsat reflectance bands was correlated to LAI. The leaf-off Landsat imagery was used because we assumed it might provide additional LAI information for understory balsam fir present in many trembling aspen stands at this site.

We did not assess quantitatively the accuracy of the two LAI maps. We present them in this study as potential ways to obtain a spatial estimate of LAI and are used here for comparison purposes only. However, the range and distribution of LAI in both maps appear reasonable compared to the LAI from the plot data and LAI data from Fassnacht et al. (1997).

Table 3
Error matrix for the ATLAS land cover classification with agreement statistics (overall accuracy=84%, kappa statistic=0.79)

Reference plots

	Aspen	Forested wetland	Northern hardwood	Red pine	Upland conifer	Open wetland	Grass/shrub	Urban	Water	Cropland	Total	Producer accuracy (%)	User accuracy (%)
Aspen	54	1	3	0	2	0	0	0	0	0	60	79	90
Forested wetland	7	85	6	0	0	1	0	0	0	0	99	93	85
Northern hardwood	4	1	58	1	1	0	0	0	0	0	65	81	89
Red pine	1	1	0	9	1	0	0	0	0	0	12	56	75
Upland conifer	1	2	4	6	5	0	0	0	0	0	18	55	27
Open wetland	0	1	0	0	0	11	0	0	0	0	12	91	91
Grass/shrub	1	0	0	0	0	0	10	0	0	0	11	100	90
Urban	0	0	0	0	0	0	0	0	0	0	0	*	*
Water	0	0	0	0	0	0	0	0	0	0	0	*	*
Cropland	0	0	0	0	0	0	0	0	0	0	0	*	*
Total	68	91	71	16	9	12	10	0	0	0	277		

2.11. NPP

NPP for each combination of LAI and land cover map (NPP$_{XZ}$) was calculated using the following equation (Fig. 2):

$$NPP_{XZ} = \varepsilon_X\, f_{APAR}\, PAR_{GS} \qquad (3)$$

where X denotes the land cover map used, Z denotes the LAI map used, ε_X is the land cover specific LUE factor (Table 2), f_{APAR} was determined using Eq. (2) and the LAI map where $k=0.57$, and PAR$_{GS}$ represents a growing season sum taken from Ahl et al. (2004). PAR$_{GS}$ was calculated from daily incident PAR by using air and soil temperature constraints on photosynthesis. We used a soil temperature (at 10 cm depth) and daily minimum air temperature threshold of 0 °C to determine the number of growing season days. Temperature measurements were obtained from each of the three micrometeorological stations (upland deciduous, upland coniferous, lowland deciduous) and used according to the dominant leaf habit (land cover type deciduous or evergreen) and topographic position (upland or wetland). For mixed stands, we determined the proportion of leaf area for each leaf habit, and modified LAI accordingly. The forested wetlands class contained 53% deciduous leaf area (mostly speckled alder) and 47% evergreen (mostly white cedar). The same procedure was used for the mixed category in the IGBP classifications. The mixed category consisted of 73% deciduous and 27% evergreen leaf area. The spatial NPP maps were created using ERDAS Imagine/Modeler® software (ERDAS, Inc, 2000, Atlanta) to process the input maps, LUE, and PAR data using Eq. (3).

2.12. Statistical analyses

We generated a random sample of 2500 locations within the site to compare mean NPP estimates. We chose 2500 as the sample size to ensure an adequate number of points per land cover class (Congalton, 1991). Using the random locations, we extracted the NPP values from each NPP map except for scenario MA, which was excluded from analyses because it only contained one value. Statistical analyses (F and t tests) were performed using SAS/MIXED® (SAS Institute Inc., 2000) to test overall site mean NPP differences.

Table 4
Error matrix for the WISCLAND land cover classification with agreement statistics (overall accuracy=50%, kappa statistic=0.41)

Reference plots

	Aspen	Forested wetland	Northern hardwood	Red pine	Upland conifer	Open wetland	Grass/shrub	Urban	Water	Cropland	Total	Producer accuracy (%)	User accuracy (%)
Aspen	25	14	17	0	4	0	2	0	0	0	62	36	40
Forested wetland	2	42	2	0	0	1	0	0	0	0	47	46	89
Northern hardwood	22	0	47	6	1	0	2	0	0	0	78	66	60
Red pine	0	1	1	10	0	0	0	0	0	0	12	62	83
Upland conifer	5	8	2	0	3	1	2	0	0	0	21	33	14
Open wetland	2	21	1	0	1	10	0	0	0	0	35	83	28
Grass/shrub	9	4	0	0	0	0	4	0	0	0	17	40	23
Urban	3	1	1	0	0	0	0	0	0	0	5	*	*
Water	0	0	0	0	0	0	0	0	0	0	0	*	*
Cropland	0	0	0	0	0	0	0	0	0	0	0	*	*
Total	68	91	71	16	9	12	10	0	0	0	277		

Urban, water, and cropland were not sampled in the reference data but appear in the classification.

3. Results

3.1. Vegetation classification

The ATLAS classification had an 84% overall accuracy compared to the field inventory data (Fig. 5a, Table 3). Most vegetation classes had a producer's and user's accuracy greater than 75%. The greatest discrepancy in the ATLAS classification was that 38% of the upland conifer reference plots were misclassified as red pine. Of the plots classified as upland conifer, 39% were actually dominated by deciduous species or were a forested wetland. Aggregating
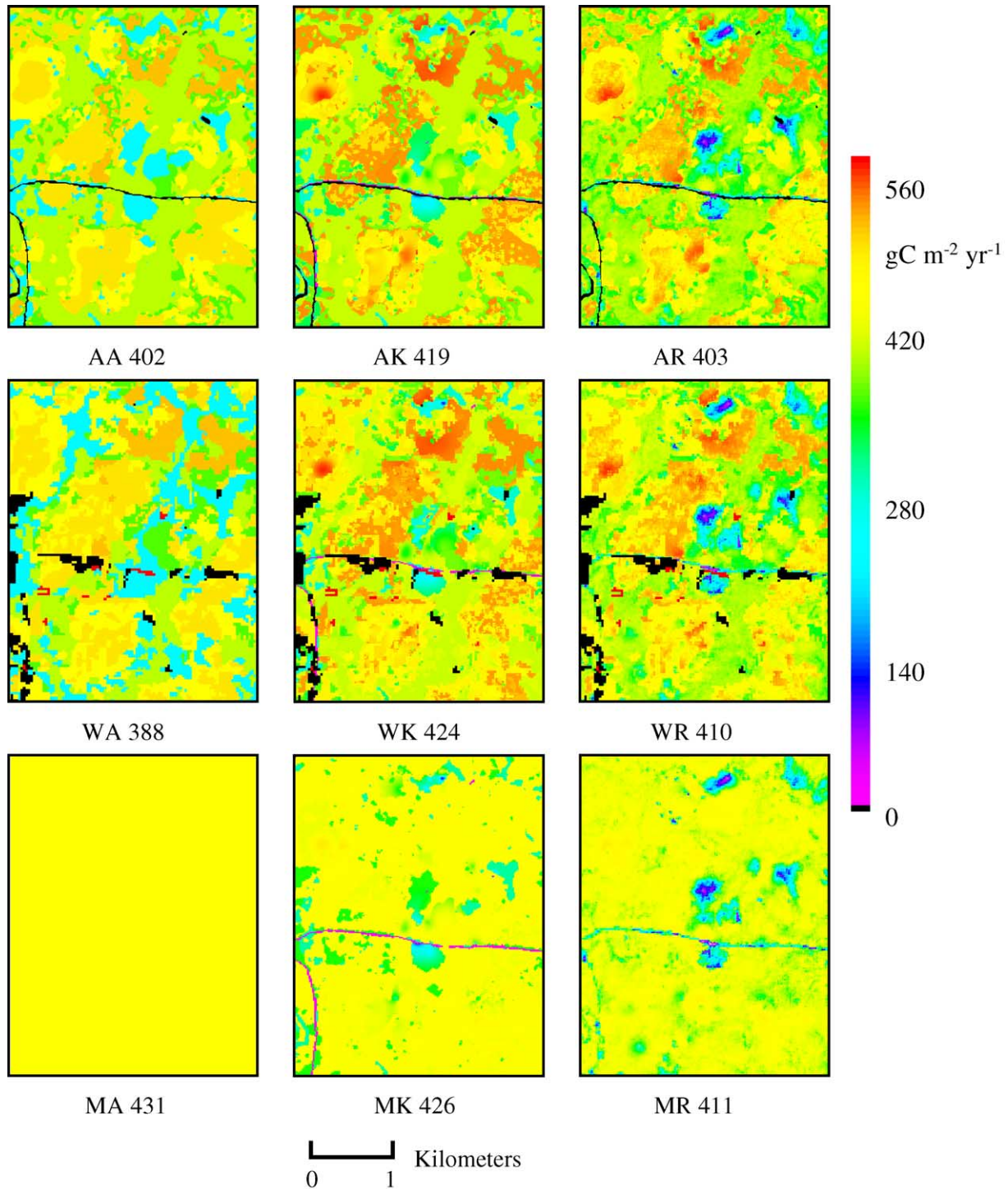

Fig. 7. Net primary production (NPP) maps derived using land cover specific light use efficiency values and spatial leaf area index (LAI) maps. Methodology and data used for each map, identified by the scenario label (AA, AK, AR...) are depicted in Fig. 2. The mean NPP (gC m^{-2} year^{-1}) for the each map is shown next to the scenario label. Differences among scenarios are described in Table 5.

Table 5
Net primary production (NPP) estimates for nine different scenarios in a 10 km^2 study area

Scenario	Sensor	Sensor resolution (m)	Mean NPP (gC m^{-2} year^{-1})	Range	% Difference
AA	ATLAS	15	402 (86)	0–505	−0.3
AK	ATLAS	15	419 (83)*	0–555	4.0
AR	ATLAS	15	403 (86)	0–560	–
WA	TM	30	388 (182)*	0–2603	−3.8
WK	TM	30	424 (165)*	0–2780	5.2
WR	TM	30	410 (164)*	0–2747	1.6
MA	MODIS	1000	431 (0)[a]	431	6.8
MK	MODIS	1000	426 (56)*	6–486	5.6
MR	MODIS	1000	411 (55)*	2–487	1.8

Differences (%) are relative to scenario AR. Mean NPP followed by one standard deviation in (). Sensor indicates the remote sensing data used to derive the land cover classification used to model NPP.
[a] Not tested due to lack of variance.
* Significantly different from AR at 95%.

red pine and upland conifer classes increased the overall, producer's, and user's accuracy to 86%, 84%, and 70%, respectively.

The overall accuracy for the WISCLAND map (derived from Landsat TM) was 50% (Fig. 5b, Table 4). Most classes had a user's and producer's accuracy less than 67%. The major misclassification problems were: 38% of the plots classified as upland conifer were forested wetlands, 60% of the plots classified as open wetland were forested wetlands, and almost 32% of the aspen plots were classified as northern hardwood. It appears from the raw imagery that some areas mapped as grass/shrub (53%) and barren (<10%) are now aspen. The WISCLAND classification identified several cropland pixels, but the inventory data and on-site visits indicated there were no cropland in this study area.

3.2. LAI and NPP

The mean LAI in 2000 calculated from all ground measurements was 3.6 (Burrows et al., 2002). The kriged and co-kriged LAI maps had a mean LAI of 3.9 and 3.4, respectively (Fig. 7).

The mean NPP differed significantly ($p < 0.001$) among all nine scenarios tested and ranged from 388 (WA) to 431 gC m^{-2} year^{-1} (MA) (Fig. 7, Table 5). Although all mean NPP comparisons differed significantly from AR, except for AA, the differences ranged only from −3.8% to 6.8%. The largest variation occurred among the WISCLAND-based scenarios because of the misclassification of cropland (high LUE) in the data. The NPP variation due to the LAI maps were apparent among the MODIS-based NPP maps.

4. Discussion

4.1. Effects of aggregation on land cover

Several studies have examined the effects of aggregating data from fine to coarse scales (Benson & MacKenzie, 1995; He et al., 2002; Steyaert et al., 1997;

Townshend & Justice, 1988; Turner et al., 1996). We did not aggregate land cover data using a neighborhood function, however, the difference in classifications between the smallest grain size (15 m) and largest grain size (1000 m) in this study corroborates results found in other studies. Benson and MacKenzie (1995) examined the effects of increasing grain size from 20 m to 1.1 km on lake parameters in northern Wisconsin and showed that as grain size increased, the number of detectable lakes decreased and the average detectable lake size increased. In our study, the number of land cover types decreased as grain increased from 15 to 1000 m. We applied a majority filter, post analysis, to the ATLAS classification to simulate a 1000 m classification, and the resultant aggregated classification contained 78% forested wetland and 22% northern hardwoods. Aggregated to the IGBP biome scale using a majority rule, this area was classified as mixed forest, similar to the MODIS classification used in the analysis.

Classifying the 15 m ATLAS data was problematic because canopy gaps and shadows created a "salt and pepper" effect in the imagery. The effect was reduced in the 30 m imagery, where stands appeared more homogeneous. Almost 27% of the error in the WISCLAND product was attributed to the fact that some of the areas have changed since the original imagery was acquired in the early 1990s. If we account for change or succession (e.g., clearcutting, regeneration, etc.), the overall agreement of the WISCLAND product improved to 77%. Thomlinson et al. (1999) suggested that overall accuracy should not be less than 85% when the land cover data will be used in validation experiments involved with EOS products. We speculate that achieving this minimum accuracy using Landsat data is possible if several classification techniques are used (e.g., Bauer et al., 1994; Stuckens et al., 2000). This would also suggest that spatial resolutions less than 30 m may not be needed for classification purposes in this area. This study highlights the growing need to classify vegetation types at scales less than 1 km^2 because most timber management units in the Chequamegon-Nicolet National Forest are smaller than this size.

4.2. Effects of land cover aggregation on NPP estimates

Past studies have shown that spatial NPP estimates were influenced significantly by grain size (e.g., Pierce & Running, 1995; Reich et al., 1999; Turner et al., 1996; Turner et al., 2002). Pierce and Running (1995) reported that NPP increased 30% as grain size increased from fine to coarse grain. They attributed the difference to using averaged temperature data in the coarse grain analysis in their mountainous study area. Nungesser et al. (1999) reported that NPP increased by 27% as grain size increased from 10 and 50 km^2 for an area roughly comprising the eastern half of the United States. They concluded that the aggregation of forest types contributed to much of the difference in NPP but also noted the coarse scale temperature data contributed to the error. Turner et al. (2000) found that total NPP decreased 12% when aggregating from 25 to 1000 m resolution. They attributed this difference to errors in the land cover classification at different scales.

Our results that NPP was relatively insensitive to land cover spatial scale is consistent with Reich et al. (1999) who reported a 5% increase in NPP from 25 to 1000 m in northern Minnesota. In our study, the NPP difference between the finest grain (AR) and coarsest grain (MA) scenario was only 7%. Accounting for spatial autocorrelation in the 2500 random locations did not change the estimate significantly. Although the NPP means differed significantly in this study, the differences among the estimates are low considering it is difficult to measure NPP in the field within 20% (Nungesser et al., 1999). While the spatial NPP estimates used in this study were partitioned by land cover, the land cover was indexed to associated LUE coefficients. More work is needed to incorporate the effects of errors in field measurements and heterogeneity in underlying physiologies (e.g., species stomatal conductance rates) in scaling studies (Ahl et al., 2004; Mackay et al., 2002).

Turner et al. (2000) suggested that scale dependant errors would not be large where land cover types detectable by remote sensing have similar NPP. We speculate that the fine and coarse grain estimates of NPP in this study were similar because almost 90% of the area is forested and that average LUE may be representative of the entire area at the coarsest scale. If the study area consisted of 25% water or urban, for example, then the NPP difference between the fine and coarse grain would be almost 30%. This scenario may not be uncommon east of this study site, which has a high density of lakes (i.e., Vilas County region). Benson and Mackenzie (1995) suggested that the exclusion of many small lakes from large grain data may be problematic for ecosystem scaling studies. This suggests the need to use species level spatial information in NPP and LUE validation experiments and the need to test and optimize methods in areas with different land cover gradients that may affect mixed pixels (Reich et al., 1999; Turner et al., 2004). Therefore, the results from this study should not be extended to other areas in northern Wisconsin, but we believe the framework of methodology used in this study is applicable elsewhere.

The land cover classification process from remote sensing data represents another source of uncertainty that may contribute to NPP differences. Although the accuracy of the ATLAS classification was only 84%, most of the class confusion involved land cover with similar NPP. Therefore, the overall effect of classification error on the NPP estimate was minimal. Similarly, the effect of the low accuracy of the WISCLAND classification on NPP estimates was offset by the distribution of land cover with similar NPP. Additionally, the commission error of agriculture (i.e., agriculture has a high LUE coefficient) only comprised 5% of the total site area, therefore having a minimal effect on the mean NPP. We suggest that future studies incorporate classification error in NPP estimates especially in NPP heterogeneous areas.

4.3. Effects of LAI on NPP estimates

The three different methods for representing spatial LAI had different effects on the landscape NPP estimates. The decrease in the NPP estimate from MA to MR reflects the variation in the LAI data because the land cover is constant in each of those scenerios. The MA scenario is informative as an aggregate LAI because it was derived from the average LAI for the mixed land cover class. We resampled the co-krige LAI map to 1000 m grain size and calculated NPP based on the LUE coefficient for the mixed class. The NPP estimate derived from the 1000 m resampled LAI was 409 gC m^{-2} year^{-1}, or only 1% different from scenario AR (Table 5). The mean NPP would be 416 gC m^{-2} year^{-1} if we used the average LAI for the entire site with the ATLAS land cover classification. Therefore, the LAI and the land cover each account for almost 50% of the total difference between the fine and coarse grain mean NPP estimate, depending on how land cover (and the LUE coefficient) is specified and how LAI is represented. Although we did not assess the accuracy of the LAI maps, we speculate that the co-kriged map may provide a better estimate of the variation of LAI because of the NDVI information that was used. The NDVI provided an additional spatial source of information regarding the leaf area, which was absent from first krige method. The difficulty with using NDVI (or other vegetation indices) alone is that LAI values greater than five in this region are difficult to predict due to sensor saturation (Fassnacht et al., 1997). The errors in field LAI data ranged from 0.4 to 1.0 m^2 m^{-2} (Burrows et al., 2002; Fassnacht et al., 1997).

At the time of this writing the average LAI and FPAR for this site derived from the Collection 4 (V004) MOD15 1 km product were 5.5 m^2 m^{-2} and 0.85, respectively. While using the MOD15 LAI would overestimate relative NPP at this site, use of FPAR directly would yield a NPP estimate similar to the 1000 m resampled LAI. It is beyond the scope

of this paper to discuss or validate the methods behind the MOD15 products. We suggest that more work is needed to explore how geostatistics may be used in combination with field data and remote sensing to adjust for the variability in LAI (Burrows et al., 2002).

4.4. Implications for validating and modeling NPP

MODIS data and process models will be used to estimate global NPP of terrestrial ecosystems (Running et al., 1999). This study shows that MODIS data may not capture the heterogeneity of land cover in some areas, but the implications for estimating NPP appear small for the region examined in this study. Results from this study and others (e.g., Nungesser et al., 1999; Turner et al., 2000) suggest that scaling and validation experiments need to use a tiered or stratified approach appropriate for the region of interest. Additional studies may be essential to stratify regions on the Earth for modeling purposes relative to the importance of spatial resolution to that region (Turner et al., 2000; Turner et al., 2004). The errors that can result from aggregating fine scale land cover information may be reduced by using partitioning (Rastetter et al., 1992) based on land cover types. The validation of NPP at fine scales is still needed in many areas in order to understand the underlying mechanisms associated with ecosystem processes, particularly where biophysical (e.g., land cover) or environmental (e.g., temperature) gradients exist. Dismissing the variability in vegetation patterns can cause variability of estimates in modeling atmospheric CO_2 (Bonan, 1995). The effects of spatial scale of data used in biogeochemical models may also depend upon which ecosystem model is used because models differ in their logic used to estimate NPP and the sensitivity of NPP to resource availability (e.g., water and nutrient availability).

5. Conclusions

Land cover information derived from remotely sensed data is an important component used in estimating NPP from local to global scales. The development of a variety of remote sensing systems with different spatial resolutions over the last several years has provided the opportunity to study the effects of sensor resolution, or scale, on land cover classifications and NPP estimates. More work is needed to examine the causes of NPP variability and to examine aggregation errors in other areas where land cover heterogeneity exists. Significant findings from this study include:

- Aggregating land cover information from fine to coarse scale had a relatively minimal effect on estimating mean NPP.
- LAI aggregation and partitioning based on land cover had a relatively minimal effect on estimating mean NPP.

- In regions where the NPP is similar despite land cover heterogeneity, it may be possible to estimate NPP reliably using biome-level land cover data (~1 km) and associated LUE estimates without incurring large errors (<10%).

References

Ahl, D. E., Gower, S. T., Mackay, D. S., Burrows, S. N., Norman, J. M., & Diak, G. (2004). Heterogeneity of light use efficiency in a northern Wisconsin forest: Implications modeling net primary production with remote sensing. *Remote Sensing of Environment*, *93*, 168–178.

Barish, L. S., & Meloy, P. E. (2000). *Wisconsin blue book 1999–2000*. Madison: Wisconsin Legislative Reference Bureau.

Bartelink, H. H., Kramer, K., & Mohren, G. M. J. (1997). Applicability of the radiation-use efficiency concept for simulating growth of forest stands. *Agricultural and Forest Meteorology*, *88*, 169–179.

Bauer, M. E., Burk, T. E., Ek, A. R., Coppin, P. R., Lime, S. D., Walsh, T. A., et al. (1994). Satellite inventory of Minnesota forest resources. *Photogrammetric Engineering and Remote Sensing*, *60*, 287–298.

Benson, B. J., & MacKenzie, M. D. (1995). Effects of sensor spatial resolution on landscape structure parameters. *Landscape Ecology*, *10*, 113–120.

Bonan, G. B. (1995). Land atmosphere interactions for climate system models—coupling biophysical, biogeochemical, and ecosystem dynamical processes. *Remote Sensing of Environment*, *51*, 57–73.

Brannon, D. P., Hill, C. L., Davis, B. A., & Birk, R. J. (1994). Commercial remote sensing program. *Photogrammetric Engineering and Remote Sensing*, *60*, 317–330.

Burrows, S. N., Gower, S. T., Clayton, M. K., Mackay, D. S., Ahl, D. E., Norman, J. M., et al. (2002). Application of geostatistics to characterize LAI for flux towers to landscapes. *Ecosystems*, *5*, 667–679.

Burrows, S. N., Gower, S. T., Norman, J. M., Diak, G., Mackay, D. S., Ahl, D. E., et al. (2003). Spatial variability of aboveground net primary production for a forested landscape in northern Wisconsin. *Canadian Journal of Forest Research*, *33*, 2007–2018.

Campbell, G. S., & Norman, J. M. (1998). *An introduction to environmental biophysics*. New York, USA: Springer-Verlag New York.

Choudhury, B. J. (2001). Estimating gross photosynthesis using satellite and ancillary data: Approach and preliminary results. *Remote Sensing of Environment*, *75*, 1–21.

Congalton, R. G. (1991). A review of assessing the accuracy of classifications of remotely sensed data. *Remote Sensing of Environment*, *37*, 35–46.

Coops, N. C., Waring, R. H., & Landsberg, J. J. (1998). Assessing forest productivity in Australia and New England using a physiologically-based model driven with averaged monthly weather data and satellite-derived estimates of canopy photosynthesis capacity. *Forest Ecology and Management*, *104*, 113–127.

Cramer, W., Kicklighter, D. W., Bondeau, A., Moore, B., Churkina, C., Nemry, B., Ruimy, A., & Schloss, A. L. (1999). Comparing global

models of terrestrial net primary productivity (NPP): Overview and key results. *Global Change Biology*, *5*(Suppl. 1), 1–15.

Cressie, N. A. (1993). *Statistics for spatial data*. New York, New York: John Wiley and Sons, Inc.

Davis, K. J., Bakwin, S., Yi, C., Berger, B. W., Zhao, C., Teclaw, R. M., et al. (2003). The annual cycles of CO_2 and H_2O exchange over a northern mixed forest as observed from a very tall tower. *Global Change Biology*, *9*, 1278–1293.

Ewers, B. E., Mackay, D. S., Ahl, D. E., Burrows, S. N., Samanta, S. S., & Gower, S. T. (2002). Tree species effects on stand transpiration in northern Wisconsin. *Water Resources Research*, *38*(7).

Fassnacht, K. S., & Gower, S. T. (1997). Interrelationships among the edaphic and stand characteristics, leaf area index, and aboveground net primary production of upland forest ecosystems in north central Wisconsin. *Canadian Journal of Forest Research*, *27*, 1058–1067.

Fassnacht, K. S., Gower, S. T., MacKenzie, M. D., Nordheim, E. V., & Lillesand, T. M. (1997). Estimating leaf area index of north central Wisconsin forests using the Landsat Thematic Mapper. *Remote Sensing of Environment*, *61*, 229–245.

Foley, J. A., Prentice, N., Ramankutty, N., Levis, S., Pollard, D., Sitch, S., et al. (1996). An integrated biosphere model of land surface processes, terrestrial carbon balance, and vegetation dynamics. *Global Biogeochemical Cycles*, *10*, 603–628.

Franklin, S. E., Lavigne, M. B., Deuling, M. J., Wulder, M. A., & E.R. Hunt, J. (1997). Landsat TM derived forest covertypes for modelling net primary production. *Canadian Journal of Remote Sensing*, *23*, 243–251.

Goetz, S. J., & Prince, S. D. (1998). Variability in carbon exchange and light utilization among boreal forest stands: Implications for remote sensing of net primary production. *Canadian Journal of Forest Research*, *28*, 375–389.

Gower, S. T., Kucharik, C. J., & Norman, J. M. (1999). Direct and indirect estimation of leaf area index, fapar, and net primary production of terrestrial ecosystems. *Remote Sensing of Environment*, *70*, 29–51.

Gower, S. T., & Norman, J. M. (1991). Rapid estimation of leaf area index in conifer and broad-leaf plantations. *Ecology*, *72*, 1896–1900.

GES Data and Information Services Center. (2005). Homepage http://daac.gsfc.nasa.gov. Last accessed 1 June 2005.

He, H. S., Ventura, S. J., & Mladenoff, D. J. (2002). Effects of spatial aggregation approaches on classified satellite imagery. *International Journal of Geographical Information Science*, *16*, 93–109.

Jakubauskas, M. E. (1996). Canonical correlation analysis of coniferous forest spectral and biotic relations. *International Journal of Remote Sensing*, *17*, 2323–2332.

Landsberg, J. J., & Gower, S. T. (1997). *Application of physiological ecology to forest management*. San Diego: Academic Press.

Lillesand, T. J., Chipman, J., Nagel, D., Reese, H., Bobo, M., Goldman, R. (1998). *Upper Midwest Gap Analysis Program Image Processing Protocol*. Environmental Management Technical Center report EMTC-98-G001, Environmental Management Technical Center, US Geological Survey, Onalaska, Wisconsin.

Lillesand, T. M., & Keifer, R. W. (2000). *Remote sensing and image interpretation*. New York: John Wiley & Sons, Inc.

Mackay, D. S., Ahl, D. E., Ewers, B. E., Gower, S. T., Burrows, S. T., Samanta, S., et al. (2002). Effects of aggregated classifications of forest composition on estimates of evapotranspiration in a northern Wisconsin forest. *Global Change Biology*, *8*, 1253–1265.

Medlyn, B. E. (1998). Physiological basis of the light use efficiency model. *Tree Physiology*, *18*, 167–176.

Milne, B. T., & Cohen, W. B. (1999). Multiscale assessment of binary and continuous landcover variables for MODIS validation, mapping, and modeling applications. *Remote Sensing of Environment*, *70*, 82–98.

Monteith, J. L. (1972). Solar radiation and productivity in tropical ecosystems. *Journal of Applied Ecology*, *9*, 747–766.

Monteith, J. L. (1977). Climate and the efficiency of crop production in Britain. *Philosophical Transactions of the Royal Society of London. Series B*, *281*, 277–294.

Myneni, R. B., & Williams, D. L. (1994). On the relationship between FAPAR and NDVI. *Remote Sensing of Environment*, *49*, 200–211.

Nungesser, M. K., Joyce, L. A., & McGuire, A. D. (1999). Effects of spatial aggregation on predictions of forest climate change response. *Climate Research*, *11*, 109–124.

Pierce, L. L., & Running, S. W. (1995). The effects of aggregating sub-grid land surface variation on large-scale estimates of net primary production. *Landscape Ecology*, *10*, 239–253.

Pinheiro, J. C., & Bates, D. M. (2000). *Mixed-effects models in S and S-PLUS*. New York, New York: Springer-Verlag New York, Inc.

Rastetter, E. B., King, A. W., Cosby, B. J., Hornberger, G. M., O'Neill, R. V., & Hobbie, J. E. (1992). Aggregating fine-scale ecological knowledge to model coarser-scale attributes of ecosystems. *Ecological Applications*, *2*, 55–70.

Reich, P. B., Turner, D. P., & Bolstad, P. (1999). An approach to spatially distributed modeling of net primary production (NPP) at the landscape scale and its application in validation of EOS NPP products. *Remote Sensing of Environment*, *70*, 69–81.

Running, S. W., Baldocchi, D. D., Turner, D. P., Gower, S. T., Bakwin, P. S., & Hibbard, K. A. (1999). A global terrestrial monitoring network integrating tower fluxes, flask sampling, ecosystem modeling and EOS satellite data. *Remote Sensing of Environment*, *70*, 108–127.

Running, S. W., & Hunt Jr., E. R. (1993). Generalization of a forest ecosystem process model for other biomes, BIOME-BGC, and an application for global-scale models. In J. R. Ehleringer & C. B. Field (Eds.), *Scaling physiological processes: Leaf to globe* (pp. 141–158). San Diego: Academic Press.

Running, S. W., Justice, C. O., Solomonson, V., Hall, D., Barker, J., Kaufmann, Y. J., et al. (1994). Terrestrial remote sensing science and algorithms planned for EOS/MODIS. *International Journal of Remote Sensing*, *15*, 3587–3620.

Running, S. W., Peterson, D. L., Spanner, M. A., & Teuber, K. B. (1986). Remote sensing of coniferous forest leaf area. *Ecology*, *67*, 273–276.

Sader, S. A., Ahl, D. E., & Liou, W. S. (1995). Accuracy of Landsat-TM and GIS rule-based methods for forest wetland classification in Maine. *Remote Sensing of Environment*, *53*, 133–144.

SAS Institute Inc. (2000). Cary, South Carolina, USA.

Sellers, P. J., Los, S. O., Tucker, C. J., Justice, C. O., Dazlich, D. A., Collatz, G. J., et al. (1996). A revised land-surface parameterization (SiB2) for atmospheric GCMs: Part 2. The generation of global fields of terrestrial biophysical parameters from satellite data. *Journal of Climate*, *9*, 706–737.

Spanner, M. A., Johnson, L., Miller, J., McCreight, R., Freemantle, J., Runyon, J., et al. (1994). Remote sensing of seasonal leaf area index across the Oregon transect. *Ecological Applications*, *4*, 258–271.

Steyaert, L. T., Hall, F. G., & Loveland, T. R. (1997). Land cover mapping, fire regeneration, and scaling studies in the Canadian boreal forest with 1 km AVHRR and Landsat TM data. *Journal of Geophysical Research*, *102*, 29581–29598.

Stuckens, J., Coppin, P. R., & Bauer, M. E. (2000). Integrating contextual information with per-pixel classification for improved land cover classification. *Remote Sensing of Environment*, *71*, 282–296.

Thomlinson, J. R., Bolstad, P. V., & Cohen, W. B. (1999). Coordinating methodologies for scaling landcover classifications from site-specific to global: Steps toward validating global map products. *Remote Sensing of Environment*, *70*, 16–28.

Townshend, J. R. C., & Justice, C. O. (1988). Selecting the spatial resolution of satellite sensors required for global monitoring of land transformations. *International Journal of Remote Sensing*, *9*, 187–236.

Turner, D. P., Cohen, W. B., & Kennedy, R. E. (2000). Alternative spatial resolutions and estimation of carbon flux over a managed forest landscape in Western Oregon. *Landscape Ecology*, *15*, 441–452.

Turner, D. P., Cohen, W. B., Kennedy, R. E., Fassnacht, K. S., & Briggs, J. M. (1999). Relationships between leaf area index and Landsat TM

spectral vegetation indices across three temperate zone sites. *Remote Sensing of Environment*, *70*, 52–68.

Turner, D. P., Dodson, R. D., & Marks, D. (1996). Comparison of alternative spatial resolutions in the application of a spatially distributed biogeochemical model over complex terrain. *Ecological Modeling*, *90*, 53–67.

Turner, D. P., Gower, S. T., Cohen, W. B., Gregory, M., & Maiersperger, T. K. (2002). Effects of spatial variability in light use efficiency on satellite-based NPP monitoring. *Remote Sensing of Environment*, *80*, 397–405.

Turner, D. P., Ollinger, S. V., & Kimball, J. S. (2004). Integrating remote sensing and ecosystem process models for landscape-to region-scale analysis of the carbon cycle. *BioScience*, *54*, 573–584.